

Determination of Stator Temperature Profile using Distributed Sensing

Hudon, C.⁽¹⁾, Lévesque, M.⁽¹⁾, Zou, L.⁽²⁾, and Picard, J.⁽¹⁾

⁽¹⁾ Institut de recherche d'Hydro-Québec, IREQ
1800 boul. Lionel-Boulet, Varennes, Québec
J3X 1S1, Canada

⁽²⁾ OzOptics Ltd.
219 Westbrook Road, Ottawa, Ontario
K0A 1L0, Canada

Abstract— The aging of generators is intimately associated with the hotspot temperature of the stator windings groundwall insulation. Common resistive thermal detectors (RTD) installed in the machine are well suited to monitor temperature changes and trends during normal operation, as long as temperature distribution is uniform, but are blind to some hotspots. Moreover, the relationship between the RTD temperature and the one of the copper conductor depends on the operating condition, the machine design and its cooling system so a simple rule of ten degree of difference is not always valid. When generators are operated close to their limit, it is essential to determine as precisely as possible the exact hotspot temperature to prevent any life reduction of the equipment. To optimize generation without any life reduction, Hydro-Quebec Research institute IREQ has been developing over the past decade a generator model that includes finite element modeling of electromagnetism, thermal, mechanical and fluid dynamics of the cooling air. This model relies on experimental data from the field to validate calculation. One of the main sensors used to validate thermal simulation is an optic fiber installed in the stator core's vent ducts. This sensor is used for distributed temperature sensing (DTS) measurement. This paper presents the comparison of the thermal model calculations, the DTS measurements and other sensors used to measure temperature in five case studies on actual generators.

Index Terms— Generator, distributed temperature sensing, thermal simulation, hotspot.

I. INTRODUCTION

In times when economic incentives drive power utilities to maximize the output of existing generators by pushing them to their limit, a better knowledge of actual temperature distribution in the entire generator is mandatory. To improve the evaluation of the hotspot temperature in generator, Hydro-Quebec's research institute has been developing over the past decade a detailed numerical model [1] to calculate temperature distribution everywhere in the machine. This model considers electromagnetic modeling of magnetic and stray losses in the stator and rotor [2]. RI² losses in the conductors are easily calculated and an estimation of windage losses and cooling air flow is obtained by computational fluid dynamics (CFD) [3]. The combination of all losses and cooling is not trivial, and finite element modeling is able to give detail information on temperature distribution everywhere in the generator. However, the results obtained from these models must always be confronted with experimental data to make sure that they reflect reality.

Even though the common RTD installed at mid-height in twelve of several hundreds of slots of the stator of hydro-generators are well suited to monitor temperature in between top and bottom bars, they only offer partial information on temperature and circumferential uniformity distribution, and no indication on the axial and radial temperature distribution. It should be reminded that RTD is a resistance, thus it integrates the average resistance along its active length (generally in the range of 50 cm) and is unable to differentiate between a uniform and non-uniform temperature distribution along its length. In addition, it is almost blind to any hotspots located some distance away from its active part. Ideally, it's the copper temperature that should be monitored to know the exact hotspot temperature, but this direct measurement is not possible with conventional sensors because the conductors are at high voltage. There has been some attempt in the past [4] to install fiber optic in close contact with the conductors inside bars and this work has revealed that an axial temperature variation of 15°C, cannot be detected by the RTD.

In order to try to get an axial temperature distribution in existing stator, we have started to test a commercial DTS system to measure the air temperature using a continuous optic fiber installed as a continuous loop in the stator cooling ducts. This

information added to the one of other sensors such as thermocouples installed at different locations in the generator is used to validate the 3D thermal mapping obtained by simulation. Here, only results from the stator are reported, even though the rotor is also covered by the model.

A sensitivity study modeling different loss distributions, published earlier [5], revealed that the RTD's reading was almost the same when top and bottom bar were at the same temperature or when there was 18°C of difference between them. This study clearly showed the limitation of the RTD to estimate the actual copper temperature. In the current paper, the temperature computed by the model will be compared with DTS measurements in the stator vent ducts and thermocouples installed in the machine to make sure that simulations are in agreement with actual behavior of the generator. The results will focus on the evaluation of the hotspot temperature and will compare it to the temperature obtained from the RTD for five case studies of actual generators evaluated during heat run test. The authors recognize that in some conditions and for some design, the rotor will be more stressed thermally than the stator. However this paper will only focus on the stator portion of the model.

II. INSTRUMENTATION OF GENERATOR FOR CASE STUDIES

The complete instrumentation during heat run test to validate simulation results requires more than 250 sensors of temperature, airflow, voltage, current, strain and acceleration. To measure the temperature distribution, a single multimode optic fiber is installed in loop in the cooling vent ducts of the stator core and is used as distributed sensor for the DTS measurement system. This measurement is not a point measurement but rather detects the temperature of the fiber all along its length. The working principle relies on Raman backscattering. The commercial instrument used in our case studies, sends series of light impulses of 10 nanoseconds and measured the time of flight of the backscattered signal, to determine location. The intensity of the signal is proportional to the temperature at this location and the output is a reading of temperature as a function of the position in meter. However, one drawback of the Raman technique is that it has at best, a spatial resolution of one meter.

Depending if the generator was open or close frame, two typical installation schemes were used: circumferential or axial. In both schemes, the fiber is passed through the stator's cooling ducts from the back of the core up to the air gap then the fiber bends sharply and comes back to the same point before continuing to the next duct. Fig. 1 shows the circumferential installation (top) and the axial installation (bottom).

Normally, in the circumferential installation every duct is instrumented as illustrated in Fig. 2 for the top, the center and the bottom level. In axial scheme, the fiber is passed in each vent duct axially for one or two slot behind each heat exchanger.

Even if the DTS measurements provide a temperature reading as a function of position, it always averages up the temperature over a fiber length of 1 meter. As can be seen in Fig. 1 (top), one meter corresponds to about one round trip of the fiber in one duct plus two times the length at the back of the core from one duct to the next. In addition, since it is not possible with this measurement to know exactly where the meter begins and end, we have built in our thermal model the calculation of a one meter average, thus it is possible to calculate a minimum and maximum temperature giving the spread of all possible values depending on the average length and the measured one must be included in this range for the model to be valid.

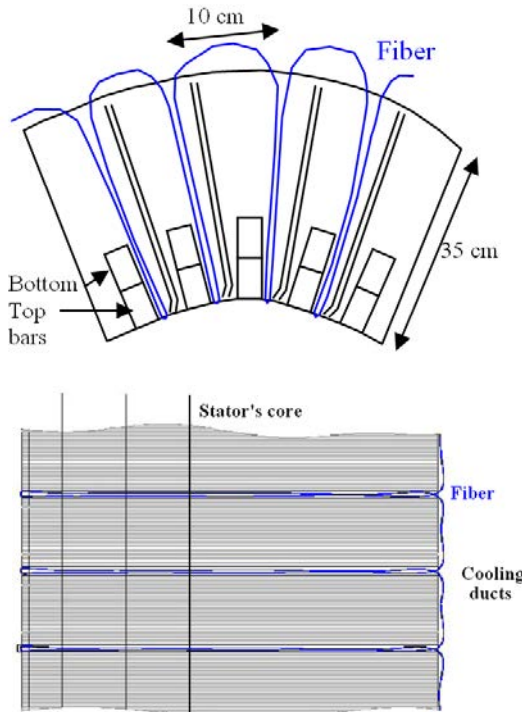


Figure 1. Circumferential installation of the fiber at every slot of one height of the stator (top) or in every duct along one slot in the axial installation (bottom).

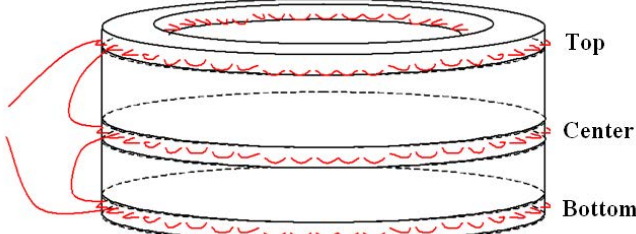


Figure 2 Circumferential installation of the fiber at three heights in the stator vent ducts..

Thermocouples installed in the machine are also used to validate simulation results. An overview of the thermocouple locations on solid surface and in air is presented by the dots in Fig. 3. In this figure, the DTS fiber in an axial configuration appears in the stator core and the RTD location is illustrated by the strait vertical line in the middle of the stator core.

III. CASE STUDY

After validation of all measurement points in every heat run test condition, we have extracted the stator's hotspot temperature from the temperatures calculated by the thermal model for each of the five generators presented in Table 1. Generators from cases B and C are in the same plant but unit C was rewound. Case B had twelve parallel circuits per phase, of multturn coils, whereas case C had Roebel bars with three parallel circuits per phase. In each case study, the temperature was calculated at every element of the 3D mesh: in the stator core, the insulation, the copper and in the cooling air. Knowing the location of the RTD and its length, it is possible to calculate the temperature it would read in the model, the one of the DTS fiber and the hotspot temperature. The measured DTS temperature is compared with the one of the air in the model over the one meter average.

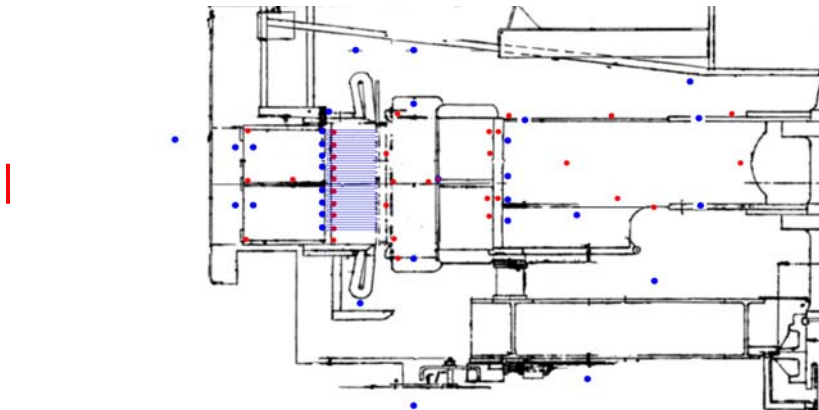


Figure 3 Example of the cross-section of a generator and location of thermocouples on solid surfaces and in air (dots).

Table I Generator characteristics and type of DTS installation

Unit	Rating (MVA)	Stator winding	RTD temperature limit (°C)	DTS installation scheme
A	65	Coil	115	Axial
B	122,6	Coil	90	Circumferential
C	122,6	Bar	110	Axial
D	184	Bar	105	Axial
E	310	Bar	105	Axial

Before comparing calculations and measurements obtained from the DTS and the RTD, thermocouple measurement points were used to make sure that the model was coherent in the no load condition and at three different loads during the heat run tests. Once all measurements points have been shown to be in agreement with simulation in every operating condition, we considered the model to be representative of the behavior of the generator. Some examples of this comparison are provided in the next section.

IV. RESULTS OF SIMULATIONS AND MEASUREMENTS

The comparison of all measurement points obtained by the thermocouples (See Fig. 3) with the calculated temperature mapping of the entire generator far exceeds the scope of this paper, but some example are given to illustrated the type of validation done. In parallel with testing, calculation with the thermal model generates a temperature map as the one in Fig. 4. Here only two half slots with core, vent ducts, bars and insulation are illustrated. At this stage, the model considers uniform condition for all angular coordinates and continuity of the geometry shown is assumed. The calculated temperature map is then used to extract temperature at each of the location where thermocouples were installed in the machine. For instance, the temperature of the air measured at the back of the core, just at the exit of eight of the vent ducts in unit A (see Table I), are compared with the simulated axial temperature profile at the exit of every duct as shown in Fig. 5. The vertical axis in this figure correspond to the position of the vent duct with vent number one being on the connection end of the machine, here at the top end. The shape of the measured axial ventilation profile for unit A is in good agreement with the simulated one in every condition: No load excited, 70%, 85% and 100% of full load. The average difference between measurements and simulations is less than 1.7°C. All other temperature sensors were also close to simulated values.

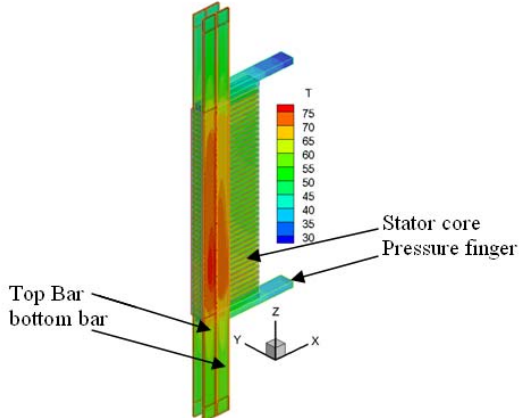


Figure 4: Example of thermal mapping from the model for unit C at nominal load.

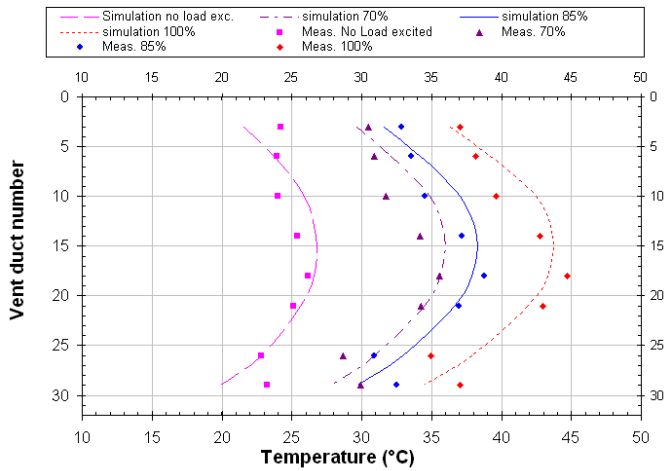


Figure 5 Comparison of measured air temperature at the exit of the stator ducts (dots) and simulation (lines) of unit A.

As can be seen for this case, the temperature is warmer in the center of the machine and becomes cooler at both ends. At nominal load the difference between the coolest end and the warmest point is in the range of 9°C. In this case, the highest temperature is at mid length of the slot where the RTDs are, so the difference between these sensors and the hotspot is expected to be smaller than for the case of unit B in Fig. 6 where the results obtained from the DTS measurements in circumferential installation indicate that the lowest temperature was at mid height in the stator.

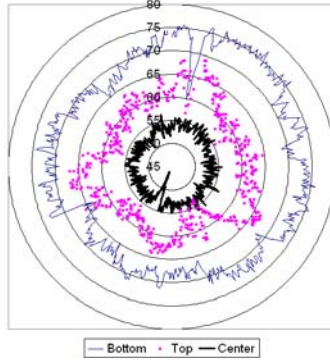


Figure 6 Temperatures from the DTS measurements in the circumferential installation of unit B at 147 MVA.

A similar validation was made for unit C between the DTS measurements and simulations of the air inside the vent ducts. As shown in Fig. 7, again the general shape of the calculated and simulated axial temperature profile is similar in every test condition. Here, it is the bottom part of the machine that was the warmest with a temperature difference of 7.5°C between the minimum and maximum at 100% of nominal load. In this machine four slots were instrumented with the DTS fiber in the axial scheme (along slots 95, 96, 155 and 156). The fiber was passed inside each of the 38 cooling ducts and the measured curves in Fig. 7 are the average of the four slots. The agreement between the model and measurements was again acceptable with differences of less than 2.5°C up to 120% of nominal load. In this case, test above nominal voltage was possible because the cooling water temperature was of 6°C .

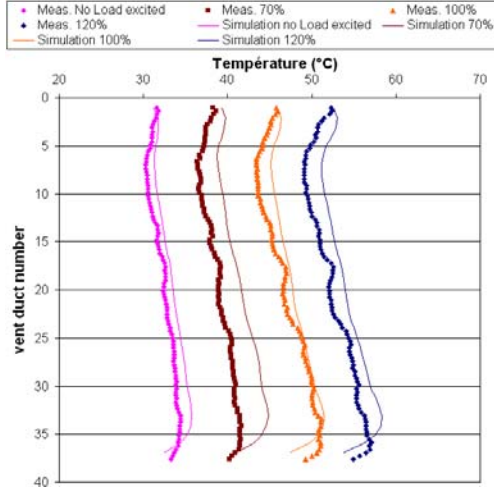


Figure 7: Comparison of the air temperature inside the vent ducts measured with the DTS fiber (dots) and simulation (lines) of unit C.

The individual temperature readings of each fiber show that the circumferential uniformity is acceptable as indicated by the temperature of the four fibers at 100% in Fig. 8. In every location, the temperature was higher toward the bottom of the stator core and the lowest temperature was located around vent duct number 6. Above this position, in vent ducts 5 to 1, the temperature of the air increased again toward the top end of the stator.

Once all measurement points including the DTS, proved that the simulation from the model was representative of reality, the measured RTD temperature can be compared with the calculated hotspot temperature. The results are shown in Table II for the five units studied.

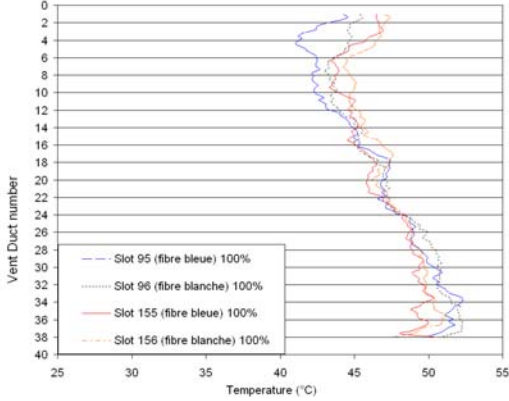


Figure 8 DTS fiber temperature at 100% of nominal load, for unit C.

Table II Comparison of the average RTD and the hotspot temperatures at or close to nominal load

Unit	RTD Measured (°C)	RTD calculated(°C)	Hotspot calculated (°C)	ΔT (°C) $T_{\text{Hotspot}} - T_{\text{RTD meas}}$
A	61.7	64.3	68.8	7.1
B	70.0	69.6	92.0	22.0
C	59.7	60.7	64.3	4.6
D	90.8	90.2	96.4	5.6
E	73.3	75.9	89.9	16.6

Temperatures and the spread between the hotspot and the RTD depends on operating conditions, on the insulation type and thickness, on the cooling water temperature, on the distribution of magnetic and stray losses, but also on the distribution of windage losses and the distribution of air in the machine. The temperature difference shown in Table II will increase with load but will also depend on the machine's design. During winter, when the water of the cooling circuit of hydro-generator is colder the machine can operate at 10 to 15% above the nominal rating so the hotspot temperature must be evaluated up to this load, but it is usually during summer that machine runs the warmest. Thus, not only the difference between the RTD and hotspot must be evaluated at a given time, but also the actual temperature of the cooling water.

V. DISCUSSION

The temptation to operate generators to higher loads usually increases with the electricity market value. However, the long term reliability of the asset assumes that the hotspot temperature is not exceeded. In order to evaluate the hotspot temperature, the best way would be to measure directly the conductor of the stator winding as in [4], however this is not currently available for existing generators. Since the difference between the RTD and the hotspot temperature is clearly dependent on the machine's design, a more thorough evaluation of the actual thermal behavior of a generator based on modeling and/or detailed measurements is recommended. To benefit from a greater flexibility of operation, the uncertainty associated with the actual hotspot temperature must be reduced as much as possible. Once this difference is determined, then the RTD can be used more adequately to operate at high loads.

When the machines are well designed and their cooling is uniform, the difference between the RTD and the actual hotspot of the copper conductor can be in the range of 5°C, as in the case of units C and D above. However, in some cases this difference can be quite significant. For instance, in the case of unit B where axial ventilation was highly non-uniform the hotspot manifested toward the bottom of the stator core as seen on the DTS results in Fig. 6, with more than 20°C of difference with the measured RTD (see Table II). Here, it was clear that the RTD located at mid-height in the core, was blind to the hotspot.

The temperature difference between the RTD and the calculated hotspot can be anything from 4 to 20°C and even larger, depending on the machine's design, the location of the RTD in the slot vs. the one of the hotspot and the uniformity of the cooling. Obviously, when the axial ventilation profile is non-uniform over the height of the stator core, the hotspot temperature could be significantly different from the one of the RTD.

Manufacturers will guarantee long term reliability when nameplate ratings are respected, but contractual guarantees usually expire after five years. In most cases, machines reach their expected end of life, but in some cases where anomalies are found, associated with non-uniform cooling for instance, premature failure and refurbishment can occur before this time. With the market pull toward short term benefits, the percentage of generator at risk may increase, so a greater need to understand the exact thermal behavior of each generator's design is needed.

Better knowledge of thermal behavior can be achieved by generator modeling, but all hypothesis used in such models have a

direct impact on the calculated location and magnitude of the hotspot, and must be validated by measurements. Improved measurements on generators with tools such as the DTS system but also better means of evaluation of the airflow in the cooling circuit (rim ducts, stator, air gap, airflow into pit...) are mandatory to feed the models. Up to now it is clear that the DTS measurements still brings more detailed information than traditional RTD, which makes calculation of the hotspot more precise.

The measurement of the axial temperature profile in the stator has proven to be an essential validation point of the model because it integrates the temperature of the stator winding, of the core and of the air in the vent ducts. However, one major drawback of the Raman DTS system, that still has to be overcome, is the 1 meter limit of the spatial resolution. At present this has been circumvented by introducing the response of the sensor into the program of our finite element model, but improve resolution is desirable. Recently, a new instrument relying on Brillouin backscattering, instead of Raman, has been developed and could improve this limit. Preliminary tests carried out in our lab on a full height stator core, with this new instrument indicate that a spatial resolution of 10 cm can be achieved. The greatest limitation of most DTS system, in our test condition, is the signal loss at every sharp fiber bend. Our laboratory test of the new instrument, with one full slot instrumented (including 20 bends), was made at room temperature. To test the spatial resolution, the fiber exiting from the core was passed over a 10 cm heating plate at 60°C. In Fig. 9, the magnitude of the temperature peak recorded by the Brillouin DTS system was of 34.8°C above ambient (slightly below the pad temperature) but did have a 10 cm width. The new instrument could improve the resolution of future field measurements, but remains to be tested in operating conditions.

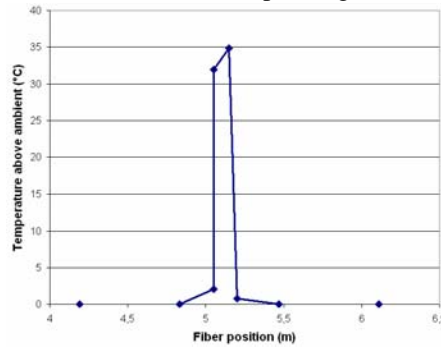


Figure 9 Spatial resolution of the Brillouin backscattering instruments.

VI. CONCLUSION

It was shown that it is not possible to determine the hotspot temperature of the stator winding based only on the RTD's reading. The best way to get this information is to combine generator modeling and *in-situ* measurements. A tool such as the DTS measurement system complement well the battery of other sensors in order to determine the exact temperature mapping of the generator. Soon tests will be made on a generator to see if a measurement can be made with a 10 cm resolution with a Brillouin DTS system on actual generators.

REFERENCES

- [1] Hudon,C., Merkhouf,A. Chaaban,M., Bélanger,S., Torriano,F., Leduc,J., Lafleur,F., Morissette,J.-F., Millet,C. and Gagné,M., "Hydro-Generator Multi-Physic Modeling", European Journal of Electrical Engineering, Vol 13, No. 5-6, 2010, pp. 563-589.
- [2] Hudon, C., Merkhouf, A. and Chaaban, M., "Consideration of Loss Distribution to evaluate the Hotspot Temperature when Up-rating Generators", IEEE Int. Symp. on Electr. Insul., San Diego, June 6-9 2010.
- [3] Toussaint, K., Torriano, F., Morissette, J.-F. and Claude Hudon, "CFD analysis of ventilation flow for a scale model hydro-generator", ASME Power 2011.
- [4] Satake, Y., Hattori, K. and Takahshi, K., "Temperature of Turbo-Generator Strands", CIGRE SC-A1 Colloquium on new developpement of rotating Electric, machines, 11-13 Sept. 2011, Beijing.
- [5] Hudon, C., Merkhouf, A. and Chaaban, M., "Consideration of Loss Distribution to evaluate the Hotspot Temperature when Up-rating Generators", IEEE Int. Symp. on Electr. Insul., San Diego, June 6-9 2010.
- [6] Chaaban, M., Leduc, J. et Hudon, C., "Thermal analysis of Large Hydro-Generator based on a multi-physic approach", CIGRE Colloquium on Rotating Machine, Beijing, China, Sept. 11~13th, 2011.